Journal of Brilliant Engineering 2 (2024) 4912
Brilliant Engineering
journal home: www.acapublishing.com/journals/4/ben
Research Article

Evaluation of Rain Attenuation Models for 5G Frequencies: Regions in Turkey

Beyza Nur Zegerek,[1], Bülent Çavuşoğlu[1]
[1]Department of Electrical-Electronics Engineering, Atatürk University, Erzurum, Turkey

Keywords

5G Frequencies,
Rain attenuation,
Satellite System.

Abstract

Rain attenuation in 5G satellite communications needs to be considered in planning the communication settings due to the fact that it causes significant attenuation especially above 10 GHz and in low elevation angle Earth-space connection paths. Even though various rain attenuation models have been developed by using measured meteorological data, it is important to know especially which model provides better results for 5G frequencies since direct satellite communication over 5G channels is planned to be used in the near feature. Hence, in this study, prominent rain attenuation models such as the Simple Attenuation Model, Garcia-Lopez model, and ITU-R P.618-14 model were examined. Using these models, rain attenuations occurring at elevation angles of 30°, 60°, and 85° were identified in three different cities in Turkey. Average annual precipitation data from the General Directorate of Meteorology of Turkey for the years 1930-2023 were utilized. The studies on various rain models using different parameters revealed that the attenuation in the 470-780 MHz frequency band is 2.849x10-4 dB, whereas there is a 12.63 dB attenuation in the range of 40.5-43.5 GHz. It was observed that the attenuation increases further with frequencies above 43.5 GHz. Therefore, it is evident that rain attenuation is a crucial parameter in satellite communication systems, particularly in 5G and beyond. This study has revealed that ITU-R P.618-14 model is the best suitable one for high elevation angles and at high frequencies (above 40GHz). As for lower elevation angles Garcia model is more appropriate.

1. Introduction

In the planning of Earth-space links for communication systems, it is crucial to consider various factors. These factors include absorption, scattering and polarization effects caused by atmospheric water and ice particles such as clouds and rainfall, as well as absorption in atmospheric gases [1]. During rainfall, significant attenuations occur in microwave and millimeter-wave communications systems, particularly in satellite communication systems operating at high-frequency bands above 10 GHz [2][3]. Therefore, precise forecasting is crucial for predicting rain-related signal weakening in microwave satellite and terrestrial direct line connections [4].

Several models have been proposed to predict rain-induced attenuation, differing in parameters like geographical locations, conditions [5]. Therefore, the most prediction models employ semi-empirical approaches, which consider two primary factors: the rainfall rate at a specific point on the Earth's surface and the effective distance over which uniform rainfall distribution is assumed [6][7].

In this study, a Simple Attenuation Model, Garcia-Lopez Model, ITU-R P.618-14 Model is investigated. The annual rainfall data acquired from the General Directorate of Meteorology of Turkey for the provinces of Igdır, Istanbul, and Rize in Turkey were analyzed at various elevation angles to observe rain attenuation rates.

2. Literature review

The specific attenuation γ_R (dB/km) is derived from R(mm/h) using the power law as shown in Equation 1. The coefficients k and α are defined as functions of frequency, f (GHz) [8].

$$\gamma_R = kR^{\alpha} \quad (1)$$

The following parameters are required for rain attenuation prediction models:

$R_{0.01}$: Rainfall rate corresponding 0.01% of the average yearly rainfall for the location (mm/h)

H_S: Earth station height above mean sea level (km)

θ: Elevation angle of the earth station (degrees)

φ: Latitude of the earth station (degrees)

f: frequency(GHz)

R_e: Effective radius of the Earth (8500 km)

The short, medium and long-term spectrum range for 5G services in satellite communication systems are presented in Table 1. This article focuses on studies conducted within these frequency ranges.

Table 1.Frequency bands planned for 5G services[9]

Short Term	Medium Term	Long Term
694-790 MHz		
2.6 GHz	1427-1518 MHz	470-694 MHz
3.6 GHz	40.5-43.5 GHz	2.3-2.4GHz
26 GHz	26 GHz	
66-71GHz		

2.1. Simple rain attenuation model

The model proposed by Stutzman and Dishman [12] was specifically developed for designing millimeter-wave satellite communication systems and accurately predicting rain-induced attenuation, as expressed in Equation 2.

Corresponding Author: beyza.zegerek@atauni.edu.tr
Received 24 May 2024; Revised 26 Jul 2024; Accepted 26 Jul 2024
https://doi.org/10.36937/ben.2024.4912

$$A = \frac{\gamma\left[1 - \exp\left(-\gamma b \ln\left(R_{0,01}/10\right)\right) L_s \cos\theta\right]}{\gamma b \ln(R_{0.01}/10) L_s \cos\theta} \quad (2)$$

Where L_S is the inclined path length given by Equation 3.

$$L_s = \frac{H_R - H_s}{\sin\theta} \qquad \theta \geq 5° \quad (3)$$

Here, H_R represents the rain height, Hs denotes the station height, and θ (in degrees) signifies the elevation angle between the horizontal projection and the slant path and the b value was optimized using the expanded database, resulting in an optimal value of b = 1/14 [10].

The rain height, H_R can be obtained from Equation 4.

$$H_R = \begin{cases} 4.8 & |\varphi| \leq 30° \\ 7.8 - 0.1|\varphi| & |\varphi| > 30° \end{cases} \quad (4)$$

2.2. Garcia-Lopez model

The Garcia Lopez model, represented by Equation 5, has been validated through testing on 77 satellite connections across Europe, the USA, Japan, and Australia. This model was developed to satisfy specific criteria identified for rain attenuation prediction methods in satellite radio link engineering [11].

$$A = \frac{\gamma L_s}{[a + (L_s(bR + cL_s + d)/e)]} \quad (5)$$

The rain height, H_R can be calculated using Equation 6:

$$H_R = \begin{cases} 4 & 0 < |\varphi| < 36° \\ 4 - 0.075(|\varphi| - 36°) & |\varphi| \geq 36° \end{cases} \quad (6)$$

The coefficients *a, b, c,* and *d* are constants that generally vary depending on the geographical area and established using regression techniques with simultaneous measurements of rain attenuation and rain rate. The coefficient *e* functions solely as a scaling factor. By choosing $e=10^4$, the coefficients considered as 'worldwide' are as follows: a=0.7, b=18.35, c=-16.51, d=500 [12].

2.3. ITU-R P.618-14 model

This model computes rain attenuation based on long-term statistics of rain attenuation along inclined paths at a specific location, covering frequencies up to 55 GHz [13]. The first step of the ITU-R P.618-14 rain attenuation model involves determining the rain height H_R according to Recommendation ITU-R P.839, which is based on the latitude of the ground station. The mean rain height above mean sea level, H_R can be derived from the 0°C isotherm using Equation 7 [14].

$$H_R = h_0 + 0.036 \quad (7)$$

The horizontal projection of L_G is calculated from the inclined path, as depicted by Equation 8:

$$L_G = L_S \cos\theta \quad (8)$$

Equation 9 provides the horizontal reduction factor:

$$r_{0,01} = \frac{1}{1 + 0.78\sqrt{\frac{L_G \gamma_R}{f}} - 0.38(1 - e^{-2L_G})} \quad (9)$$

The vertical adjustment factor, $v_{0.01}$ for 0.01% of the time is determined using Equation 10, 11, 12 and 13.

$$\zeta = \tan^{-1}\left(\frac{H_R - H_S}{L_G r_{0,01}}\right) \quad (10)$$

If ζ>0,

$$L_R = \frac{L_G r_{0,01}}{\cos\theta} \quad (\text{km}) \quad (11)$$

Else,

$$L_R = \frac{(H_R - H_S)}{\sin\theta} \quad (12)$$

If φ<36° then χ=36-|φ| otherwise χ=0

$$v_{0.01} = \frac{1}{1 + \sqrt{\sin\theta}\left(31(1 - e^{-(\theta/(1+\chi))})\frac{\sqrt{L_R \gamma_R}}{f^2} - 0.45\right)} \quad (13)$$

Equation 14 calculates the effective path length as follows:

$$L_E = L_R v_{0.01} \quad (14)$$

Equation 15 the predicted attenuation exceeding 0.01% of the average yearly value.

$$A_{0,01} = \gamma L_E \quad (15)$$

Here, p represents the desired percentage of an average year other than 0.01%, while β is the coefficient calculated based on the φ and θ values. The specific value of β is detailed in Table 2, which lists the parameters upon which it depends.

Table 2. Percentage of time, relationship between β, φ, θ

p≥1% or |φ|≥36°	$\beta = 0$
p<1% and |φ|<36° and θ≥25°	$\beta = -0.005(\|\varphi\| - 36)$
Otherwise	$\beta = -0.005(\|\varphi\| - 36) + 1.8 - 4.25\sin\theta$

Equation 16 provides the rain attenuation.

$$A_p = A_{0.01}\left(\frac{p}{0.01}\right)^{-(0.655 + 0.033\ln(p) - 0.045\ln(A_{0.01}) - \beta(1-p)\sin\theta)} \quad (16)$$

3. Simulation

The evaluated models were analyzed using the MATLAB platform. Precipitation data between 1930 and 2023 were taken from the Turkish Meteorology Directorate [15]. Table 3 presents the data required to evaluate rain attenuation models in the mentioned cities.

Table 3. The data to be used in attenuation models for the referenced cities

City	Average Annual Accumulation mm/year	$R_{0.01}$ mm/hr.	Station Height km	Latitude φ
Igdır	258.4	64.08	0.85	39.895802°
Istanbul	662.5	84.78	0.04	41.046419°
Rize	2300	122.74	0.006	41.025113°

The simulations were conducted using SAM, Garcia Lopez and ITU-R P.618 models at different elevation angles (θ = 30, 60, 85 degrees) with MATLAB and the resulting graphs are presented below. Figure 1 illustrates the attenuation observed at various elevation angles for the city of Igdır, where the x-axis illustrates frequency in GHz and the y-axis denotes the attenuation in dB.

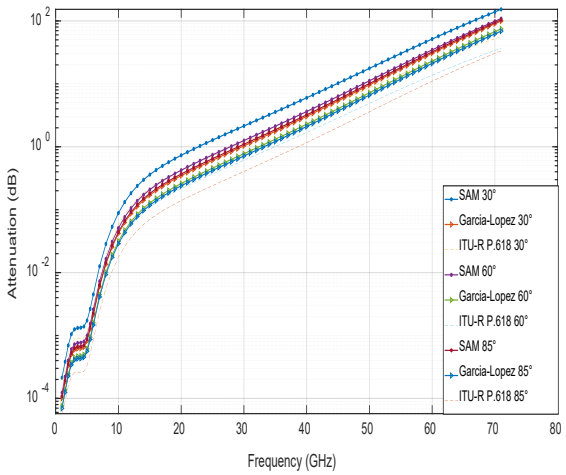

Figure 1. θ=30°, θ=60°, θ=85°Rain Attenuation for Igdır

Figure 1 demonstrates that attenuation increases with frequency. Specifically, at an elevation angle of 30°, the SAM rain attenuation model shows the highest attenuation across all frequencies, while at an elevation angle of 85°, the ITU-R P.618-14 model exhibits the lowest attenuation. The graph clearly illustrates how different elevation angles and models affect attenuation. Furthermore, despite varying attenuation values, different models exhibit similar attenuation trends. Detailed data is available in Table 4 based on Figure 1. Examination of Table 4 reveals that both the SAM model and other models show minimal attenuation within the 470-790 MHz band. As elevation angle increases, attenuation decreases. Furthermore, attenuation levels are observed to be below 10 dB in the frequency range of 40.5-43.5 GHz and lower, with significant attenuation occurring at 66 GHz and above. Analysis of rain attenuation models for the Igdır province shows that the ITU-R P.618-14 model provides the lowest attenuation levels at 85°.

The Istanbul region experiences higher precipitation compared to Igdır region, with a station altitude of 0.04 km affecting the slope (Ls). Longer paths lead to increased attenuation. The attenuation graph obtained for Istanbul is shown in Figure 2.

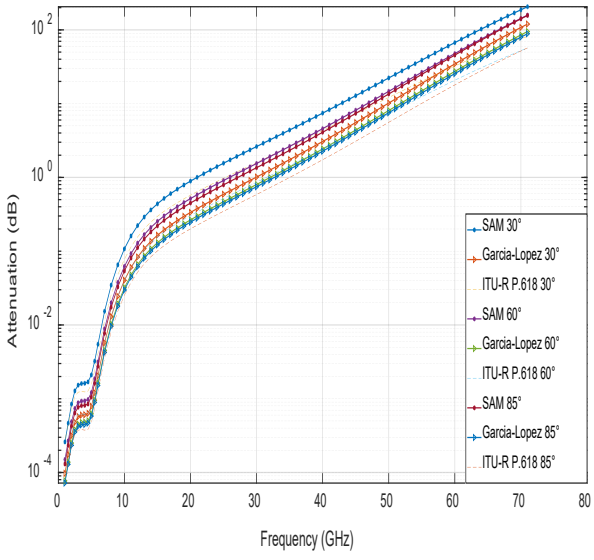

Figure 2. . θ=30°, θ=60°, θ=85°Rain Attenuation for Istanbul

In Figure 2, the SAM rain attenuation model exhibits maximum attenuation across all frequency values at an elevation angle of 30°, while the ITU-R P.618-14 rain attenuation model shows the minimum attenuation at an elevation angle of 85°. The graph demonstrates that the highest performance is achieved with the ITU-R P.618-14 model at 85°, followed by the 60° ITU-R P.618-14 model. For more detailed data, comprehensive information is available in Table 5, based on the findings from Figure 2. Although the attenuation values displayed in the SAM, Garcia-Lopez, and ITU-R P.618-14 models are higher, the graphs exhibit the same characteristics for the Igdır region. It has been noted that geographical factors, such as altitude, should also be considered when assessing the effects of decreased precipitation on satellite communication systems.

Rize, located in the northeast of Turkey, is known as the country's rainiest province due to receiving abundant rainfall throughout the year. The $R_{0.01}$ value, representing only 0.01% of the total, exceeds 122.74 mm/year. For the region of Rize, attenuation graphs of evaluated rainfall attenuation models are presented in Figure 3, while attenuation data are presented in tabular form in Table 6.

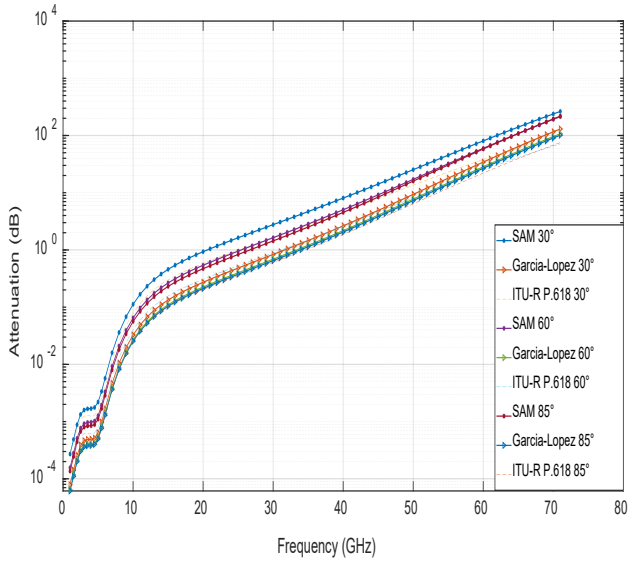

Figure 3. θ=30°, θ=60°, θ=85°Rain Attenuation for Rize

Examination of Figure 3 reveals that the attenuation values are higher compared to those in Figure 1 and Figure 2. Nonetheless, at an elevation angle of 30°, the SAM model exhibits maximum attenuation, while the best performance occurs at 85° with the ITU-R P.618-14 model. In the frequency ranges of 40.5-43.5 GHz and 66-71 GHz, the Garcia Lopez and ITU-R P.618-14 models show closely aligned attenuation values at 60° and 85° elevation angles.

In the frequency range of 40.5 GHz to 43.5 GHz, maximum attenuation of 9.185 dB is observed in Igdır province, 11.47 dB in Istanbul province, and 12.63 dB in Rize province, indicating the impact of precipitation on signal degradation. Rain serves as a significant source of attenuation in electromagnetic wave propagation, constituting one of the pivotal meteorological factors impacting its communication, notably concerning millimeter-wave frequencies exceeding 10 GHz [16]. It is observed that attenuation increases with frequency. Alongside frequency, parameters such as latitude, rainfall rate, and station altitude are determined to influence attenuation. In the context of 5G satellite communication systems, precipitation can significantly impact signal transmission by causing attenuation, particularly in higher frequency bands.

Table 4. Rain attenuation values in dB for city of Igdır

Frequency	θ	Bound	SAM	Garcia-Lopez	ITU-R P.618
470-790 MHz	30°	max	$2.136x10^{-4}$	$1.01x10^{-4}$	$1.952x10^{-4}$
	60°	max	$1.233x10^{-4}$	$7.575x10^{-5}$	$9.642x10^{-5}$
	85°	max	$1.072x10^{-4}$	$6.968x10^{-5}$	$5.725x10^{-5}$
1.427-1.518 MHz	30°	max	$6.95x10^{-4}$	$3.287x10^{-4}$	$5.248x10^{-4}$
		min	$2.136x10^{-4}$	$1.01x10^{-4}$	$1.952x10^{-4}$
	60°	max	$4.013x10^{-4}$	$2.465x10^{-4}$	$2.544x10^{-4}$
		min	$1.233x10^{-4}$	$7.575x10^{-5}$	$9.642x10^{-5}$
	85°	max	$3.488x10^{-4}$	$2.267x10^{-4}$	$1.534x10^{-4}$
		min	$1.072x10^{-4}$	$6.968x10^{-5}$	$5.725x10^{-5}$
2.3-2.4 GHz	30°	max	$1.049x10^{-3}$	$4.962x10^{-4}$	$7.622x10-^{4}$
		min	$6.95x10^{-4}$	$3.287x10^{-4}$	$5.248x10^{-4}$
	60°	max	$6.057x10^{-4}$	$3.721x10^{-4}$	$3.681x10^{-4}$
		min	$4.013x10^{-4}$	$2.465x10^{-4}$	$2.544x10^{-4}$
	85°	max	$5.266x10^{-4}$	$3.423x10^{-4}$	$2.228x10^{-4}$
		min	$3.488x10^{-4}$	$2.267x10^{-4}$	$1.534x10^{-4}$
2.6 GHz	30°	max	$1.255x10^{-3}$	$5.937x10^{-4}$	$8.818x10^{-4}$
		min	$1.049x10^{-3}$	$4.962x10^{-4}$	$7.622x10^{-4}$
	60°	max	$7.247x10^{-4}$	$4.451x10^{-4}$	$4.24x10^{-4}$
		min	$6.057x10^{-4}$	$3.721x10^{-4}$	$3.681x10^{-4}$
	85°	max	$6.3x10^{-4}$	$4.302x10^{-4}$	$2.574x10^{-4}$
		min	$5.266x10^{-4}$	$4.095x10^{-4}$	$2.228x10^{-4}$
3.6 GHz	30°	max	$1.331x10^{-3}$	$6.293x10^{-4}$	$9.026x10^{-4}$
		min	$1.319x10^{-3}$	$6.238x10^{-4}$	$8.939x10^{-4}$
	60°	max	$7.682x10^{-4}$	$4.719x10^{-4}$	$4.322x10^{-4}$
		min	$7.615x10^{-4}$	$4.677x10^{-4}$	$4.267x10^{-4}$
	85°	max	$6.678x10^{-4}$	$4.341x10^{-4}$	$2.63x10^{-4}$
		min	$6.62x10^{-4}$	$4.302x10^{-4}$	$2.6x10^{-4}$
26 GHz	30°	equal	1.418	0.6786	0.7947
	60°	equal	0.8251	0.5088	0.4082
	85°	equal	0.7197	0.4681	0.2677
40.5-43.5 GHz	30°	max	9.185	4.785	4.714
		min	6.002	3.042	3.151
	60°	max	5.654	3.588	2.581
		min	3.628	2.281	1.692
	85°	max	5.053	3.3	1.818
		min	3.217	2.098	1.166
66-71 GHz	30°	max	152.7	99.75	56.02
		min	94.81	59.46	37.88
	60°	max	108.9	74.79	36.79
		min	65.85	44.58	24.02
	85°	max	104	68.8	33.53
		min	62.16	41.01	20.66

Table 5. Rain attenuation values in dB for city of Istanbul

Frequency	θ	Bound	SAM	Garcia-Lopez	ITU-R P.618
470-790 MHz	30°	max	2.599×10^{-4}	9.726×10^{-5}	2.812×10^{-4}
	60°	max	1.5×10^{-4}	7.704×10^{-5}	1.466×10^{-4}
	85°	max	1.304×10^{-4}	7.189×10^{-5}	8.669×10^{-5}
1.427-1.518 MHz	30°	max	8.457×10^{-4}	3.165×10^{-4}	7.38×10^{-4}
		min	2.599×10^{-4}	9.726×10^{-5}	2.812×10^{-4}
	60°	max	4.883×10^{-4}	2.507×10^{-4}	3.708×10^{-4}
		min	1.5×10^{-4}	7.704×10^{-5}	1.466×10^{-4}
	85°	max	4.245×10^{-4}	2.339×10^{-4}	2.261×10^{-4}
		min	1.304×10^{-4}	7.189×10^{-5}	8.669×10^{-5}
2.3-2.4 GHz	30°	max	1.277×10^{-3}	4.777×10^{-4}	1.066×10^{-3}
		min	8.457×10^{-4}	3.165×10^{-4}	7.38×10^{-4}
	60°	max	7.37×10^{-4}	3.784×10^{-4}	5.332×10^{-4}
		min	4.883×10^{-4}	2.507×10^{-4}	3.708×10^{-4}
	85°	max	6.407×10^{-4}	3.531×10^{-4}	3.264×10^{-4}
		min	4.245×10^{-4}	2.339×10^{-4}	2.261×10^{-4}
2.6 GHz	30°	max	1.527×10^{-3}	5.716×10^{-4}	1.227×10^{-3}
		min	1.277×10^{-3}	4.777×10^{-4}	1.066×10^{-3}
	60°	max	8.818×10^{-4}	4.527×10^{-4}	6.105×10^{-4}
		min	7.37×10^{-4}	3.784×10^{-4}	5.332×10^{-4}
	85°	max	7.666×10^{-4}	4.225×10^{-4}	3.749×10^{-4}
		min	6.407×10^{-4}	3.531×10^{-4}	3.264×10^{-4}
3.6 GHz	30°	max	1.619×10^{-3}	6.059×10^{-4}	1.251×10^{-3}
		min	1.605×10^{-3}	6.006×10^{-4}	1.236×10^{-3}
	60°	max	9.347×10^{-4}	4.799×10^{-4}	6.193×10^{-4}
		min	9.265×10^{-4}	4.757×10^{-4}	6.092×10^{-4}
	85°	max	8.126×10^{-4}	4.478×10^{-4}	3.812×10^{-4}
		min	8.054×10^{-4}	4.439×10^{-4}	3.755×10^{-4}
26 GHz	30°	equal	1.73	0.6585	1.074
	60°	equal	1.01	0.5215	0.5737
	85°	equal	0.8824	0.4867	0.386
40.5-43.5 GHz	30°	max	11.47	4.909	6.527
		min	7.436	3.065	4.325
	60°	max	7.236	3.888	3.744
		min	4.577	2.428	2.428
	85°	max	6.538	3.628	2.747
		min	4.09	2.266	1.735
66-71 GHz	30°	max	206	119.8	81.62
		min	125.9	69.35	54.81
	60°	max	158.2	94.9	56.8
		min	93.45	54.93	36.83
	85°	max	156.9	88.57	56.97
		min	91.08	51.26	34.48

Table 6. Rain attenuation values in dB for city of Rize

Frequency	θ	Bound	SAM	Garcia-Lopez	ITU-R P.618
470-790 MHz	30°	max	$2.711x10^{-4}$	$7.874x10^{-5}$	$2.849x10^{-4}$
	60°	max	$1.565x10^{-4}$	$6.503x10^{-5}$	$1.466x10^{-4}$
	85°	max	$1.36x10^{-4}$	$6.136x10^{-5}$	$8.801x10^{-5}$
1.427-1.518 MHz	30°	max	$8.82x10^{-4}$	$2.562x10^{-4}$	$7.471x10^{-4}$
		min	$2.711x10^{-4}$	$7.874x10^{-5}$	$2.849x10^{-4}$
	60°	max	$5.092x10^{-4}$	$2.116x10^{-4}$	$3.758x10^{-4}$
		min	$1.565x10^{-4}$	$6.503x10^{-5}$	$1.466x10^{-4}$
	85°	max	$4.427x10^{-4}$	$1.997x10^{-4}$	$2.293x10^{-4}$
		min	$1.36x10^{-4}$	$6.136x10^{-5}$	$8.801x10^{-5}$
2.3-2.4 GHz	30°	max	$1.331x10^{-3}$	$3.867x10^{-4}$	$1.079x10^{-3}$
		min	$8.82x10^{-4}$	$2.562x10^{-4}$	$7.471x10^{-4}$
	60°	max	$7.687x10^{-4}$	$3.194x10^{-4}$	$5.402x10^{-4}$
		min	$5.092x10^{-4}$	$2.116x10^{-4}$	$3.758x10^{-4}$
	85°	max	$6.682x10^{-4}$	$3.014x10^{-4}$	$3.31x10^{-4}$
		min	$4.427x10^{-4}$	$1.997x10^{-4}$	$2.293x10^{-4}$
2.6 GHz	30°	max	$1.593x10^{-3}$	$4.627x10^{-4}$	$1.242x10^{-4}$
		min	$1.331x10^{-3}$	$3.867x10^{-4}$	$1.079x10^{-3}$
	60°	max	$9.196x10^{-4}$	$3.822x10^{-4}$	$6.183x10^{-4}$
		min	$7.687x10^{-4}$	$3.194x10^{-4}$	$5.402x10^{-4}$
	85°	max	$7.995x10^{-4}$	$3.606x10^{-4}$	$3.8x10^{-4}$
		min	$6.682x10^{-4}$	$3.014x10^{-4}$	$3.31x10^{-4}$
3.6 GHz	30°	max	$1.688x10^{-3}$	$4.905x10^{-4}$	$1.266x10^{-3}$
		min	$1.674x10^{-3}$	$4.862x10^{-4}$	$1.25x10^{-3}$
	60°	max	$9.748x10^{-4}$	$4.051x10^{-4}$	$6.272x10^{-4}$
		min	$9.663x10^{-4}$	$4.016x10^{-4}$	$6.169x10^{-4}$
	85°	max	$8.475x10^{-4}$	$3.822x10^{-4}$	$3.863x10^{-4}$
		min	$8.4x10^{-4}$	$3.789x10^{-4}$	$3.805x10^{-4}$
26 GHz	30°	equal	1.816	0.5386	1.095
	60°	equal	1.063	0.4448	0.5862
	85°	equal	0.9296	0.4197	0.3951
40.5-43.5 GHz	30°	max	12.63	4.321	7.075
		min	8.062	2.635	4.601
	60°	max	8.125	3.569	4.085
		min	5.032	2.176	2.596
	85°	max	7.404	3.368	3.023
		min	4.524	2.053	1.865
66-71 GHz	30°	max	263.4	130	100.3
		min	156.4	72.35	66.1
	60°	max	213.8	107.3	71.51
		min	122	59.76	45.38
	85°	max	218	101.3	75.27
		min	121.9	56.38	44.19

4. Results and conclusions

In this study, the attenuation effects caused by rain at different elevation angles for millimeter-wave frequencies in Igdır, Istanbul, and Rize provinces have been investigated. It has been determined that rain is a significant source of attenuation for millimeter waves above 10 GHz. The SAM, Garcia Lopez, and ITU-R P.618-14 models were employed to predict rain attenuation in this study, focusing on frequency ranges intended for 5G services. Particularly at frequencies above 40 GHz, significant increases in attenuation were observed. At higher frequencies, the increased impact of rain particles leads to greater attenuation of electromagnetic waves in rainy conditions, potentially affecting the sensitivity of communication links. In Rize, where the annual rainfall rate is highest, greater attenuation was observed compared to other locations. For instance, at 470-790 MHz frequency range and 30° elevation angle, attenuation was measured at $2.711x10^{-4}$ dB with the SAM model, whereas in Istanbul and Igdır, attenuations of $2.599x10^{-4}$ dB and $2.136x10^{-4}$ dB, respectively, were observed. These findings highlight the influence of rainfall on attenuation. Additionally, it was observed that attenuation decreases with increasing elevation angles. For example, at 30° elevation angle in Rize province, attenuation was 1.816 dB with the SAM model, compared to 0.5386 dB with the Garcia Lopez model and 1.095 dB with the ITU-R P.618-14 model at 26 GHz frequency band and at 85° elevation angle, the ITU-R model showed less attenuation compared to other models. In the 40.5-43.5 GHz frequency range, the Garcia Lopez model performed better at 30° and 60° elevation angles, whereas the ITU-R model showed superior performance at 85°elevation angle. At 66-71 GHz frequency range, reasonable results were obtained across all elevation angles with the ITU-R model. The attenuation values obtained for Rize, Igdır and Istanbul vary depending on the rainfall rate, and the attenuation prediction models exhibit consistent behavior across different frequencies, as depicted in the graphs. It was observed that the SAM model performs inadequately at high frequencies and high rainfall rates, whereas the ITU and Garcia Lopez models show comparable performance, yielding better results at high frequencies and rainfall rates. These findings underscore the significance of rain attenuation, particularly in satellite communication systems, notably within the 5G and future communication frameworks. It's imperative to factor in rain model losses alongside operational frequencies. To ensure that all allocated frequency bands for mm-wave communication in high frequencies achieve the desired performance, new scenarios need to be developed for rain attenuation models. These scenarios should consider factors such as antenna diameter, local atmospheric conditions (e.g., fog density, wind direction and magnitude), and raindrop size.

Acknowledgement

The authors would like to thank the Turkey State Meteorological Service for providing precipitation data for this research.

Declaration of Conflict of Interests

The author(s) declare that there is no conflict of interest. They have no known competing financial interests or personal relationships that could have appeared to influence the work reported in this paper.

References

[1.] A. Y. Abdulrahman, T. A. Rahman, S. K. A. Rahim, ve M. R. Ul Islam, "A new rain attenuation conversion technique for tropical regions", *Prog. Electromagn. Res. B*, c. 26, sayı 26, ss. 53–67, 2010, doi: 10.2528/PIERB10062105.

[2.] L. J. Mpoporo, P. A. Owolawi, ve A. O. Ayo, "Utilization of Artificial Neural Networks for Estimation of Slant-Path Rain Attenuation", *Proc. - 2019 Int. Multidiscip. Inf. Technol. Eng. Conf. IMITEC 2019*, ss. 1–7, 2019, doi: 10.1109/IMITEC45504.2019.9015837.

[3.] I. Afahakan, K. Udofia, ve M. Umoren, "Analysis of Rain Rate and Rain Attenuation for Earth-Space Communication Links Over Uyo - Akwa Ibom State", *Niger. J. Technol.*, c. 35, sayı 1, s. 137, 2016, doi: 10.4314/njt.v35i1.21.

[4.] J. S. Ojo ve S. E. Falodun, "NECOP propagation experiment: Rain-rate distributions observations and prediction model comparisons", *Int. J. Antennas Propag.*, c. 2012, 2012, doi: 10.1155/2012/913596.

[5.] A. Gaur ve S. K. Sharma, "Analysis of rain attenuation prediction models along earth-satellite path over Indian cities", *2017 Innov. Power Adv. Comput. Technol. i-PACT 2017*, c. 2017-Janua, sayı 2, ss. 1–6, 2017, doi: 10.1109/IPACT.2017.8245002.

[6.] J. S. Mandeep, "Prediction of Signal Attenuation due to Rain Models at Tronoh, Malaysia", *Mapan - J. Metrol. Soc. India*, c. 28, sayı 2, ss. 105–111, 2013, doi: 10.1007/s12647-013-0050-4.

[7.] A. Usha ve G. Karunakar, "Preliminary analysis of rain attenuation and frequency scaling method for satellite communication", *Indian J. Phys.*, c. 95, sayı 6, ss. 1033–1040, 2021, doi: 10.1007/s12648-020-01748-w.

[8.] ITU-R, "Recommendation ITU-R P.838-3: Specific attenuation model for rain", 2005. [Çevrimiçi]. Available at: https://www.itu.int/dms_pubrec/itu-r/rec/p/R-REC-P.838-3-200503-I!!PDF-E.pdf

[9.] B. T. V. İ. Kurumu, *Mobil Genişbant Spektrum Stratejisi*. 2019, ss. 1–5.

[10.] W. L. Stutzman ve K. M. Yon, "A simple rain attenuation model for earth-space radio links operating at 10–35 GHz", *Radio Sci.*, 1986, doi: 10.1029/RS021i001p00065.

[11.] J. A. Garcia-Lopez, J. M. Hernando, ve J. M. Selga, "Simple Rain Attenuation Prediction Method for Satellite Radio Links", *IEEE Trans. Antennas Propag.*, c. 36, ss. 444–448, 1988, doi: 10.1109/8.192129.

[12.] COST, *COST Action 255: Radiowave Propagation Modelling for SatCom Services at Ku-Band and Above*, c. 53, sayı 9. 2002.

[13.] P.618-14 International Telecommunication ve R. Sector, "International Telecommunication Union Recommendations Radiocommunication Sector Propagation data and prediction methods required for the design of Earth-space telecommunication systems", 2023. [Çevrimiçi]. Available at: https://www.itu.int/publ/R-REC/en

[14.] ITU-R, "Recommendation ITU-R P.839-3: Rain height model for prediction methods isotherm height above mean sea level", 2001.

[15.] The Turkish Meteorology Directorate, "Turkish Meteorological Directorate Official Statistics", *https://www.mgm.gov.tr/veridegerlendirme/il-ve-ilceler-istatistik.aspx*, 2024.

[16.] E. Alozie *vd.*, "A Review on Rain Signal Attenuation Modeling, Analysis and Validation Techniques: Advances, Challenges and Future Direction", *Sustain.*, c. 14, sayı 18, 2022, doi: 10.3390/su141811744.

How to Cite This Article

Zegerek, B.N., Cavusoglu, B., Evaluation of Rain Attenuation Models for 5G Frequencies: Region in Turkey, Brilliant Engineering, 2(2024), 4912. https://doi.org/10.36937/ben.2024.4912